Robustness Examination of Tracking Performance in the Presence of Ionospheric Scintillation Using Software GPS/SBAS Receiver

*Shun-Ichiro Kondo[1], Nobuaki Kubo[2], Akio Yasuda[3]

[1]Laboratory of Communication Engineering, Tokyo University of Marine Science and Technology.(E-mail: shun@denshi.e.kaiyodai.ac.jp)

[2] Laboratory of Communication Engineering, Tokyo University of Marine Science and Technology.(E-mail: nkubo@e.kaiyodai.ac.jp)

[3] Laboratory of Communication Engineering, Tokyo University of Marine Science and Technology.(E-mail: yasuda@e.kaiyodai.ac.jp)

Abstract

Ionospheric scintillation induces a rapid change in the amplitude and phase of radio wave signals. This is due to irregularities of electron density in the F-region of the ionosphere. It reduces the accuracy of both pseudorange and carrier phase measurements in GPS/satellite based Augmentation system (SBAS) receivers, and can cause loss of lock on the satellite signal. Scintillation is not as strong at mid-latitude regions such that positioning is not affected as much. Severe effects of scintillation occur mainly in a band approximately 20 degrees on either side of the magnetic equator and sometimes in the polar and auroral regions. Most scintillation occurs for a few hours after sunset during the peak years of the solar cycle. This paper focuses on estimation of the effects of ionospheric scintillation on GPS and SBAS signals using a software receiver.

Software receivers have the advantage of flexibility over conventional receivers in examining performance. PC based receivers are especially effective in studying errors such as multipath and ionospheric scintillation. This is because it is possible to analyze IF signal data stored in host PC by the various processing algorithms. A L1 C/A software GPS receiver was developed consisting of a RF front-end module and a signal processing program on the PC. The RF front-end module consists of a down converter and a general purpose device for acquiring data. The signal processing program written in MATLAB implements signal acquisition, tracking, and pseudorange measurements. The receiver achieves standalone positioning with accuracy between 5 and 10 meters in 2drms.

Typical phase locked loop (PLL) designs of GPS/SBAS receivers enable them to handle moderate amounts of scintillation. So the effects of ionospheric scintillation was estimated on the performance of GPS L1 C/A and SBAS receivers in terms of degradation of PLL accuracy considering the effect of various noise sources such as thermal noise jitter, ionospheric phase jitter and dynamic stress error.

Keywords: software GPS/SBAS receiver, ionospheric scintillation

1. Introduction

Japan has been developing its own satellite-based GPS augmentation system called MSAS (MTSAT satellite based augmentation system) since 1993 [1]. The MSAS is the Japanese version of SBAS/WAAS and is developed primarily for civil aviation purposes. It shall broadcast radio signals based on the international standard developed and defined by ICAO (international civil aviation organization). SBAS (satellite-based Augmentation system) is the ICAO standard of a wide area augmentation system which augments GPS using additional signals transmitted from geostationary satellites [2][3]. As an international standard system, Japanese MSAS is compatible with US WAAS and European EGNOS systems. SBAS receivers shall work with any of these systems.

Following the success of the MTSAT-1R launch in February 2005, the MTSAT-2 geostationary satellite was successfully launched in February 2006. MTSAT means multifunctional transport satellite. It has weather and aviation missions. For aviation users, MTSAT provides transponder channels both for satellite communications including the automatic dependent surveillance (ADS) function as well as voice, and MSAS navigation data link. MTSAT-1R and MTSAT-2 are functional on the geostationary orbit at 140E and 145E respectively. For now, MSAS is under test procedures.

A prototype L1 PC based software GPS/SBAS receiver has been developed for the test of MSAS and other researches. It was coded in MATLAB to process sampled GPS data afterward in order to study GPS signal processing and some errors such as scintillation. In a software GPS receiver, all the processing including signal acquisition, tracking, data decoding and solving position are implemented in software except down conversion of RF signal to IF (Intermediate frequency) done by RF front-end and AD conversion process. Thus the accuracy and the function are controllable according to the algorithms and parameters. A software receiver can be a powerful tool for GPS research. The ability to change low-level functionality of a GPS receiver without modifying the hardware allows rapid testing of newly developed algorithms and the use of a receiver in nontraditional ways. PC based receivers are especially suitable to study errors and test new algorithms.

Ionospheric scintillation is a rapid change in the amplitude and/or phase of the radio signal as it passes through small-scale plasma density irregularities in the ionosphere. These scintillations reduce the accuracy of both GPS/SBAS receiver pseudorange and carrier phase measurements, and can result in a

complete loss of lock on a satellite. Many researchers have analyzed the effects in this area [3], [5] and modeled the effects on GPS/SBAS reference and user receiver's performance [1].

This work is part of an effort for robustness examination of GPS/SBAS receiver tracking performance in the presence of ionospheric scintillation and to improve the availability of MSAS. The paper is organized as follows: Section 2 explains inonospheric scintillation. Section 3 indicates development progress the GPS/SBAS receiver. Section 4 shows the PLL performance degradation in a GPS/SBAS receiver due to ionospheric scintillations. In the last section, summary of this work and the future works are indicated.

2. Ionospheric Scintillation

Small scale irregularities of electron density in the F-region of the ionosphere generate amplitude and phase scintillations in GPS signals. Amplitude scintillation causes cycle slips and data loss, and phase scintillation generates fast variations of frequency. Amplitude scintillations of GPS L1 signal, of which carrier frequency is at 1.5GHz, may exceed 20dB fading for several hours particularly in post-sunset to midnight hours during solar maximum periods in the magnetic equatorial anomaly region.

Two commonly used measures of scintillation activity are the rms intensity, S_4, and the rms phase, σ_ϕ, defined as

$$S_4 = \sqrt{\frac{E\langle I^2\rangle}{E\langle I\rangle^2} - 1} \tag{1}$$

$$\sigma_\phi = \sqrt{E\langle \phi^2\rangle} = \sqrt{\int_{-\infty}^{\infty} S_{\phi_p}(f)df} \tag{2}$$

Where $E\langle\ \rangle$ denotes average, ϕ is the carrier phase, S_{ϕ_p} represents the Power Spectal Density (PSD) of phase scintillation, $I = A^2$ is the signal intensity, and A is the signal amplitude. Scintillation can be modeled as a Nakagami-m PDF for amplitude and a zero-mean Gaussian PDF for amplitude.

The three scintillation levels shown in Table.3 are considered in this paper. These levels are representative of the range of scintillation intensity that may be encountered in different regions of the world during various phases of the 11 year solar cycle and at various local times. []

Table 2. scintillation classes considered (GPS L1)

	S4	$\sigma\phi$
strong	≧ 0.9	≧ 0.8
Moderate	0.6-0.75	0.4
Very weak	≦ 0.1	≦ 0.05

3. Software receiver

The system architecture is shown in Fig.1. The receiver consists of a front end and a software signal processing module. The front end is the only hardware module in the receiver. It contains a down-converter and an ADC.

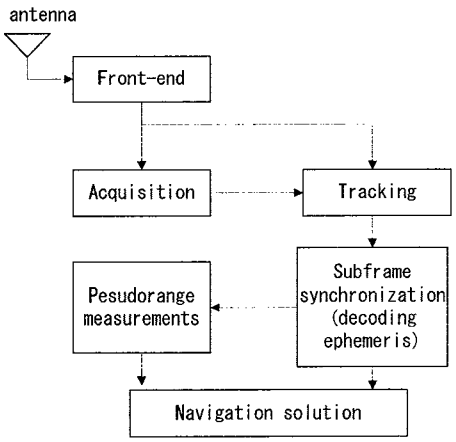

Fig.1 system architecture of the receiver

3.1 Front-end module

A down converter named 'Dual Channel Down Converter' is used in the receiver as shown in Fig.2 and its characteristics are given in table.1. It produces two IF signals at 13.99 MHz and 13.6 MHz corresponding to GPS L1 and L2 respectively. Made in Idaqs Inc, a device named PCDAQ has an ADC for general-purpose data capturing and shown in Fig.3. It uses the reference clock introduced from the down converter as an external clock to synchronize the sampling frequency with the IF signal. This is because the IF signal has frequency fluctuations due to clock jitter. The Sampling rate is variable through a synthesizer. Sampled GPS data is stored in a hard disk of 1.4TB. The characteristics are given in Table.2.

The Down converter and PCDAQ are provided by ENRI (Electronic Navigation Research Institute).All the other modules (acquisition, tracking) are implemented in another PC.

A signal processing module for L1 CA which achieves the accuracy of standalone positioning between 5 and 10 meters in 2drms has already been developed. It is coded in MATLAB and consists of acquisition, tracking, subframe synchronization, and navigation solution modules.

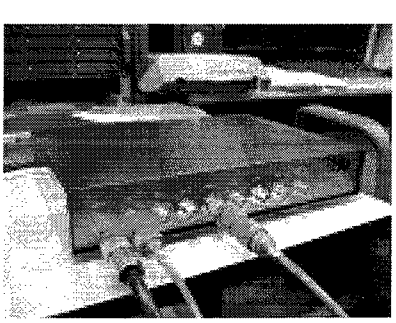

Fig.2 Dual Channel Down Converter.

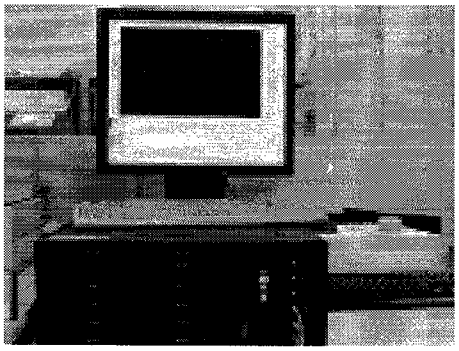

Fig.3 PCDAQ

Table 1. Characteristics of the down converter

Frequency	1.57542GHz (L1) 1.2276GHz (L2)
IF (intermediate frequency)	13.991429MHz (L1) 13.60 (L2)
Band width(IF stage)	18MHz
Gain	65dB
Reference clock	10MHz

Table 2. Characteristics of PCDAQ

Sampling frequency	Max:105MHz
Data resolution	14bit
Channels	4ch
Capacity	1.44TB

3.2 signal processing module

The Acquisition algorithm uses a FFT based method. First is coarse Acquisition to search Doppler offset and code offset. Second is Doppler refinement. In the Tracking module, 2nd order DLL is used, code tracking loop and carrier tracking loop consists of 2nd order FLL and 3rd order PLL. Carrier loop is created to coordinate tracking performance by switching between coarse FLL, refined FLL, coarse PLL and refined PLL. These techniques are introduced as shown in figure 4. These loops consist of a discriminator and loop filter. The discriminators of each loop are as follows [2].

$$\text{PLL: } \tan^{-1}\left(Q_p(t)/I_p(t)\right) \tag{3}$$

$$\text{FLL: } \frac{\tan^{-1}(cross, dot)}{t(n)-t(n-1)} \tag{4}$$

$$\text{DLL: } \frac{(I_e^2(t)+Q_e^2(t))-(I_L^2(t)+Q_l^2(t))}{(I_e^2(t)+Q_e^2(t))+(I_l^2(t)+Q_l^2(t))} \tag{5}$$

Where I, Q are prompt, early or late integration represented in Figure. 4. dot and $cross$ are

$$dot = I_p(t-1)\cdot I_p(t)+Q_p(t-1)\cdot Q_p(t) \tag{6}$$

$$cross = I_p(t-1)\cdot Q_p(t)-I_p(t)\cdot Q_p(t-1) \tag{7}$$

The transfer function of the loop filter is described as

$$F(z)=\frac{\sum_{n=0}^{N-1} b_n z^{-n}}{\left(1-z^{-1}\right)^{N-1}} \tag{8}$$

where N is the order of the carrier tracking loop. In the case of a third-order PLL (as used for the studies conducted here), the optimal coefficients of loop filters in the transfer function can be expressed as

$$b_0=\frac{T_{coh}^2\omega_0^3}{4}+\frac{a_3^{(0)}\omega_0^2 T_{coh}}{2}+b_3^{(0)} \tag{9}$$

$$b_1=\frac{T_{coh}^2\omega_0^3}{2}-2b_3^{(0)}\omega_0 \tag{10}$$

$$b_2=\frac{T_{coh}^2\omega_0^3}{4}\frac{a_3^{(0)}\omega_0^2 T_{coh}}{2}+b_3^{(0)}\omega_0 \tag{11}$$

where $a_3^{(0)}=1.1$ and $b_3^{(0)}=2.4$ [2] and ω_0 is the natural frequency of a closed-loop system. For a third-order loop, ω_0 is related to the equivalent noise bandwidth (ENB) B_n by [2]:

$$\omega_0 = B_n/0.7845 \tag{12}$$

Therefore, PLL properties will change with different ENB. While a wider bandwidth (10 Hz or more) is required for the PLL to converge, a narrower bandwidth can be used to subsequently track phase variations.

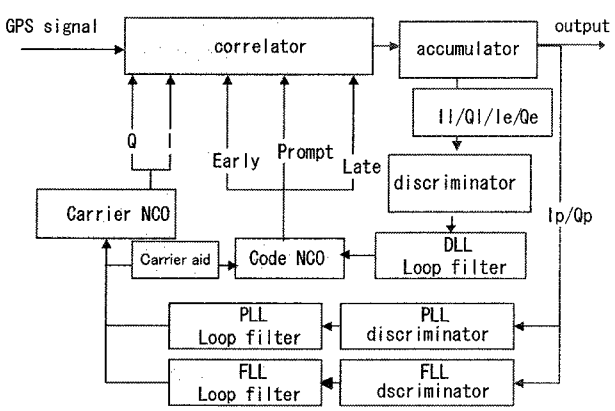

Fig.4 Architecture of Tracking loop

The Acquisition and Tracking modules correspond to GPS L1CA (PRN: 1~32) and MSAS (PRN: 129,134). Although SBAS signal can easily be acquired and tracked by a little

modification of GPS L1CA module, the encoding of the SBAS message is particularly different from the ephemeris message of L1 CA. The baseline message data rate is 250 bits per second. The data is always 1/2 convolutional encoded with a Forward Error Correction (FEC) code. Therefore, the symbol rate that the receiver must process is 500 symbols per second (sps). The convolutional coding will be constraint length 7 which is standard for Viterbi decoding, with a convolutional encoder logic arrangement as illustrated in Figure 5. The G1 symbol is selected on the output as the first half of a 4 millisecond data bit period. (If soft decision decoding is used, the bit error rate (BER) performance gain of this combination of coding and decoding is 5 dB over uncoded operation.) As an example, the algorithms for the implementation of this decoding are described in [3]. George C. Clark and J. Bibb Cain, Error Correction Coding for Digital Communications.

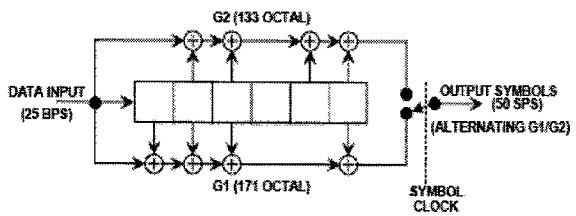

Fig.5 convolutional encoder

4. Measurement Errors

The dominant sources of phase error in PLL are phase jitter and dynamic stress. By rule of thumb of filter design, tracking threshold is designed such that 3-sigma of the phase error in PLL should not exceed 45 degrees given by [2].

$$3\sigma_{\phi,\varepsilon} = 3\sigma_{\phi,j} + \theta_e \le 45 \ \text{[deg]} \qquad (13)$$

where $\sigma_{\phi,\varepsilon}$ is the 1-sigma PLL phase jitter, $\sigma_{\phi,j}$ denotes the 1-sigma phase jitter from all sources except dynamic stress of jerk and θ_e represents the dynamic stress error in PLL. If the effects of ionospheric scintillations and thermal noise are considered in isolation, the 1-sigma phase jitter of the PLL tracking loop, $\sigma_{\phi,j}$, can be expressed with four distinct components such as a thermal noise, an ionospheric scintillation effect, a vibration induced oscillator jitter and an Allan deviation induced oscillator jitter. Hence, the resulting rule-of-thumb of PLL filter design can be rewritten by

$$\sigma_{\phi,\varepsilon} = \sqrt{\sigma_{\phi T}^2 + \sigma_{\phi s}^2 + \sigma_v^2 + \theta_A^2} + \frac{\theta_e}{3} \le 15 \ \text{[deg]} \qquad (14)$$

where $\sigma_{\phi T}$ the 1-sigma thermal noise, $\sigma_{\phi s}$ denotes the 1-sigma phase jitter from the ionospheric scintillation effect, σ_v represents the 1-sigma vibration induced oscillator jitter, and θ_A is the Allan deviation induced oscillator jitter. The units of all variables in Eq(14) are degrees.

The thermal noise jitter of PLL with the ionospheric scintillation effect on the intensity is computed as follows:

$$\sigma_{\phi,\varepsilon} = \frac{360}{2\pi}\sqrt{\frac{B_n}{c/n_0(1-S_4)}\left(1+\frac{1}{2\eta\, c/n_0(1-2S_4^2)}\right)} \ \text{[deg]} \qquad (15)$$

where B_n is the carrier loop noise bandwidth in Hz, c/n_0 denotes the carrier-to noise density power ratio ($=10^{C/N_0/10}$ for C/N_0 dBHz), η denotes the pre-detection integration time in sec and λ_L represents the wave length of L1 GPS frequency (= 0.1903 m/cycle) without scintillation effect (S_4=0), the Eq (15) becomes the standard thermal noise tracking error of PLL given by

$$\sigma_{\phi,\varepsilon} = \frac{360}{2\pi}\sqrt{\frac{B_n}{c/n_0}\left(1+\frac{1}{2\eta\, c/n_0}\right)} \ \text{[deg]} \qquad (16)$$

The PLL thermal noise jitter is often treated as the only source of carrier tracking error because the other sources of PLL jitter may be either transient or negligible. Note that the PLL thermal noise jitter is proportional to the noise bandwidth and the inverse of the predetection integration time.

The PLL phase noise from the ionospheric scintillation effect on phase is obtained from the PSD of phase scintillation modeled as $P_{\phi s}(f) = Tf^{-p}$, where T is the Spectral Strength parameter in rad2/Hz corresponding to the power at 1Hz, p denotes the slope of PSD for $f >> f_0$ which normally ranges between 2.0 and 3.0, f_0 represents the frequency corresponding to the maximum irregularity of the ionosphere in Hz. The resulting approximation is considered to be quite accurate in the effective ranges and is given as follows [1,3,4]:

$$\sigma_{\phi,\varepsilon} = \frac{360}{2\pi}\sqrt{\frac{\pi \cdot T}{k f_n^{P-1}\left(\frac{(2k+1-p)\pi}{2k}\right)}} \ \text{[deg]}, \quad \text{for } 1 < f < 2k \qquad (17)$$

where f_n is the loop natural frequency in Hz and k is the loop order. The value of T and p are recorded in the Information Systems Management Review Board (ISMRB) data log for real data cases or generated by WBMOD [10] for simulation and analysis cases. Note that $\sigma_{\phi s}$ has a constant value under T and p for the kth order filter. In this paper, its value was assumed as 5.6, 3.0-4.5 and 3.0 corresponding to strong, moderate and very weak scintillation cases as shown in Table.1.

The equation for vibration-induced Oscillator jitter is:

$$\sigma_v = \frac{360 f_L}{2\pi}\sqrt{\int_{f\min}^{f\max} S_v^2(f_m)\frac{P(f_m)}{f_m^2}\,df_m} \ \text{[deg]} \qquad (18)$$

where $S_v(f_m)$ is the oscillator vibration sensitivity of $\Delta f / f_L$ per g as a function of f_m, f_m denotes the random vibration modulation frequency in Hz and $P(f_m)$ represents the power curve of random vibration as a function of f_m in g^2/Hz.

The equation of Allan deviation oscillator phase noise jitter is calculated by using the equation for short term Allan deviation for k-th order PLL given as follows[2]:

$$\theta_{Ak} = A\frac{\sigma_A(\tau) f_L}{B_n} \text{ [deg]} \tag{19}$$

where $\sigma_{A(\tau)}$ is the short term Allan deviation [dimensionless], A denotes a constant parameter depending on the PLL order and $\tau(=1/B_n)$ represents the short term stability gate time for Allan variance measurement in seconds. For 3rd order PLL, A is equal to 160 and $\sigma_{A(\tau)}$ is given by

$$\sigma_A(\tau) = 2.25\frac{\Delta\theta}{\omega_L \tau} \text{ [deg]} \tag{20}$$

where is the rms jitter from the oscillator going into the phase discriminator in radians.

Dynamic stress error is obtained from the steady-state error formulas and depends on the loop bandwidth and the PLL order. The dynamic stress error for a 3rd order PLL is given as follows [2] :

$$\theta_{e3} = \frac{\dddot{R}}{\omega_0^3} \text{ [deg]} \tag{21}$$

where θ_{e3} denotes the 3rd order PLL dynamic stress error, $\dddot{R}$ $(=dR^3/dt^3)$ represents the maximum line-of-sight jerk dynamics in deg/sec^3 and ω_0 $(=B_n/0.7845)$ is the natural frequency of the 3rd order PLL.

The total PLL jitter as a function C/N0 for a 3rd order PLL including all effects is obtained by applying Eqs (15) (17) (18) and (19) into Eq.(14) and is indicated in Figure 6. In this figure, the noise bandwidth is assumed to be 10 Hz and four different cases of scintillations are modeled $(S_4 = 0, 0.6, 0.7 \text{ and } 0.99)$. Note that scintillation is a dominant error source in the region of low C/N0. Figure 7 shows the design margin on dynamic stress at threshold as a function of C/N0 for a 3rd order PLL with the same assumptions. The result shows that a 10 Hz noise bandwidth is available to only less than a 2.5 g/s jerk stress and this does not met the design specification of high dynamic GPS receivers. Although this condition is likely to be met when the GPS receiver is stationary, it is not guaranteed under both high dynamic environments and weak signal conditions. Figure 8 and 9 are corresponding results of an 18 Hz noise bandwidth. Note that the total PLL jitter in the case of an 18 Hz noise band width is little larger than a 10 Hz case while the dynamic robustness of the PLL is remarkably improved.

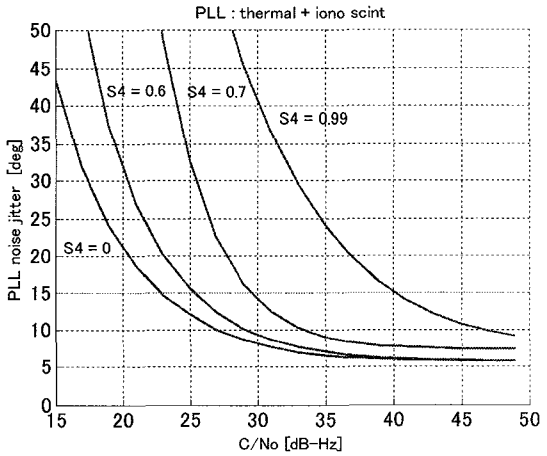

Fig.6 The total PLL jitter as a function C/N0 foe a 3rd order PLL in case of 10 Hz noise bandwidth

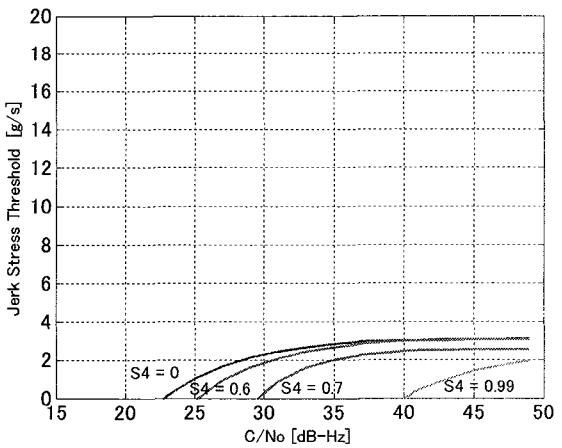

Fig.7 Dynamic stress at threshold as a function of C/N0 for a 3rd order PLL in case of 10 Hz noise bandwidth

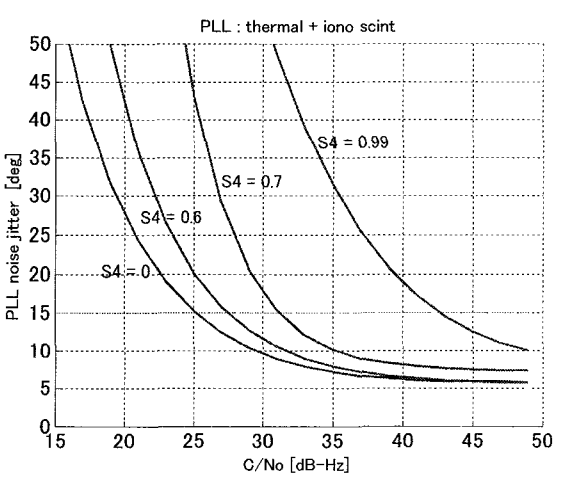

Fig.8 The total PLL jitter as a function C/N0 foe a 3rd order PLL in case of 18 Hz noise bandwidth

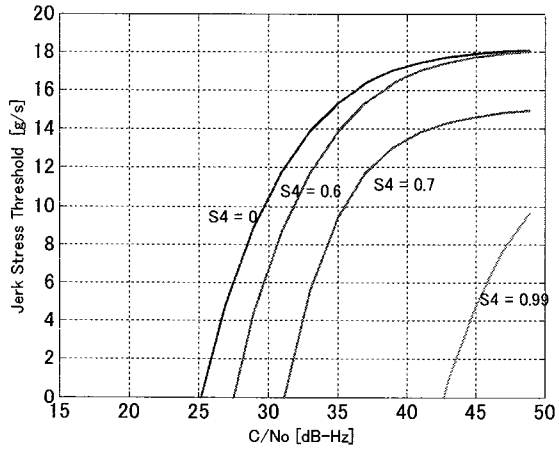

Fig.9 Dynamic stress at threshold as a function of C/N0 for a 3rd order PLL in case of 18 Hz noise bandwidth

6. Summary & Future Works

In this paper, the development progress of a GPS/SBAS receiver and the ionospheric scintillation effects on the PLL of GPS receivers were discussed. All the noise sources, such as thermal noise jitter including the effect of the intensity of ionospheric scintillation, phase jitter from the rms phase of ionospheric scintillation, vibration induced oscillator jitter, and Allan deviation induced oscillator jitter and dynamic stress error were considered and their effects on the typical 3rd order PLL were evaluated. The speculation that a 3rd order PLL on the receiver is able to accommodate line-of-sight dynamic stress of jerk by spreading the noise bandwidth of the loop filter is confirmed.

The receiver has enough availability and accuracy to examine the robustness of tracking performance in the presence of ionospheric scintillation. In addition to this evaluation, examination of the robustness using actual or simulated GPS/SBAS data signal is planned. Furthermore, the authors will try to design and implement a PLL which allows the noise bandwidth and loop order to vary to accommodate the scintillation effects and dynamic stress.

Acknowledgement

This paper was strongly inspired by the paper of Jong Hoon won [11] Fundamental hints are obtained from this paper. At the same time, the authors very much appreciate following people for support. Kazuaki Hoshinoo, Takeyasu Sakai, Keisuke Matsunaga, Minoru Ito in Electronic Navigation Research Institute (ENRI).

Reference

1. Conker, R. S., M. B. El-Arini, C. J. Hegarty and T. Hsiao, "Modeling the effects of ionospheric scintillation on GPS/SBAS availability," MP-00W0000179, Center f or Advanced Aviation System Development, the MITE R. Crop, McLean, VG, Aug2000.
2. Kaplan, E. D., "Understanding GPS: Principles and A pplications," Artech House Publishers, 1996.
3. Hegarty, C., El-Arini, M.B., Kim, T. and S. Ericson, "Scintillation modeling for GPS Wide Area Augmentati onSystem receivers", *Radio Science*, Vol. 36, No. 5, September/October 2001.
4. Knight, M. and A. Finn, A. "The effects of ionospheri c scintillations on GPS "*Proceedings of the ION GPS 1998*, Nashville, Tennessee, September, 1998.
5. Arons, J and Basu, S., "Ionospharic Amplitude and Pha se Fluctuations at the GPS Frequencies," *Proceedings of the ION GPS-1994,* Slat Palace Convention Center, Salt Lake City, UT, Sept. 20-23, 1994, pp.1569-1578.
6. George C. Clark and J. Bibb Cain, "Error Correction Coding for Digital Communications", Plenum Press, N ew York, 1981.
7. Pullen, S., Opshaug, G., Hansen, A., Walter, T., Enge, P. and B. Parkinson, B., "A preliminary study of the effect of ionospheric scintillation on WAAS user availa bility in equatorial regions," *Proceedings of the ION G PS 1998*, Alexandria, VA, September, 1998
8. Skone, S., and K. Knudsen, Impact of ionospheric scin tillations on SBAS performance, *Proceedings of the IO N GPS 2000*, Salt Lake City, UT, September, 2000.
9. Skone. S, Lachapelle. G, Yao. D, Yu. W and Watson, R, " Investigating the Impact of Ionospheric Scintillati on Using a GPS Software Receiver, " *Proceedings of ION GNSS 18th International Technical Meeting of the Satellite Division,* 13-16 September 2005, Long Beach, CA pp.1126-1137.
10. Secan, J. A., *WBMOD: Ionospheric Radiowave Scintill ation Model*, Version 13.04, Northwest Research Assoc iates, Inc., Bellevue, Wash., 1996.
11. J. H. Won, K. Hoshinoo, "Acquisition and Tracking Meth ods for a very Weak GPS signal", The 11th Winter Ins titute Report, JISTEC.